

Ring-shaped dysphotopsia associated with posterior chamber phakic implantable collamer lenses with a central hole

Youngsub Eom,¹ Dae Wook Kim,² Dongok Ryu,^{3,4,5} Jun-Heon Kim,⁶ Seul Ki Yang,^{3,4,5} Jong Suk Song,¹ Sug-Whan Kim^{3,4,5} and Hyo Myung Kim¹

¹Department of Ophthalmology, Korea University College of Medicine, Seoul, South Korea

²College of Optical Sciences, University of Arizona, Tucson, Arizona, USA

³Space Optics Laboratory, Department of Astronomy, Yonsei University, Seoul, South Korea

⁴Center for Galaxy Evolution Research, Yonsei University, Seoul, South Korea

⁵Yonsei University Observatory, Yonsei University, Seoul, South Korea

⁶Joeunnun Vision Clinic, Seoul, South Korea

ABSTRACT.

Purpose: To evaluate the incidence of central hole-induced ring-shaped dysphotopsia after posterior chamber phakic implantable collamer lens (ICL) with central hole (hole ICL) implantation and to investigate the causes of central hole-induced dysphotopsia.

Methods: The clinical study enrolled 29 eyes of 15 consecutive myopic patients implanted with hole ICL. The incidence of ring-shaped dysphotopsia after hole ICL implantation was evaluated. In the experimental simulation study, non-sequential ray tracing was used to construct myopic human eye models with hole ICL and ICL without a central hole (conventional ICL). Simulated retinal images measured in log-scale irradiance were compared between the two ICLs for an extended Lambertian light-emitting disc object 20 cm in diameter placed 2 m from the corneal vertex. To investigate the causes of hole-induced dysphotopsia, a series of retinal images were simulated using point sources at infinity with well-defined field angles (0 to -20°) and multiple ICL models.

Results: Of 29 eyes, 15 experienced ring-shaped dysphotopsia after hole ICL implantation. The simulation study using an extended Lambertian source showed that hole ICL-evoked ring-shaped dysphotopsia was formed at a retinal field angle of $\pm 40^\circ$. Component-level analysis using a well-defined off-axis point source from infinity revealed that ring-shaped dysphotopsia was generated by stray light refraction from the inner wall of the hole and the posterior ICL surface.

Conclusion: Hole ICL-evoked ring-shaped dysphotopsia was related to light refraction at the central hole structure. Surgeons are advised to explain to patients the possibility of ring-shaped dysphotopsia after hole ICL implantation.

Key words: central hole – dysphotopsia – posterior chamber phakic implantable collamer lenses

Acta Ophthalmol.

© 2016 Acta Ophthalmologica Scandinavica Foundation. Published by John Wiley & Sons Ltd

doi: 10.1111/aos.13248

Introduction

The posterior chamber phakic implantable collamer lens (ICL) has been

successfully used for correction of moderate-to-high myopia (Sanders et al. 2003; Alfonso et al. 2011).

Implantable collamer lens (ICL) has the advantage of being reversible through ICL exchange. However, ICL requires preoperative laser iridotomy or intraoperative peripheral iridectomy to prevent pupillary block. There is also a risk of cataract formation due to direct contact of the ICL with the crystalline lens or poor circulation of aqueous humour (Gonvers et al. 2003; Fujisawa et al. 2007).

A new-generation ICL with a central hole (hole ICL) was developed to overcome the disadvantages of conventional ICL. Previous studies have demonstrated that hole ICL can provide similar optical performance to that of the conventional ICL (Shiratani et al. 2008; Uozato et al. 2011; Kamiya et al. 2013; Perez-Vives et al. 2013). However, hole ICL has the potential to evoke problematic dysphotopsia caused by stray light interaction with the hole structure. Recently, a 21-year-old female patient who underwent hole ICL implantation at our institute reported glare and ring-shaped dysphotopsia (Fig. 1). Ring-shaped dysphotopsia was easily observed especially when the patient stared at a bright light.

Non-sequential ray tracing provides a comprehensive evaluation of optical system performance, including the various effects of stray light deviation from the nominal ray path (Donnelly 2008). Thus, the non-sequential

approach was used in this study to model the light source, human eye and ICL in a single unified simulation platform called the ADVANCED SYSTEMS ANALYSIS PROGRAM (ASAP™, Breault Research Organization, Inc., Tucson, AZ, USA).

This study comprised two parts, a clinical study and an experimental simulation study. The clinical study was performed to evaluate the incidence of ring-shaped dysphotopsia after hole ICL implantation. The experimental simulation was conducted to investigate the causes of hole-induced ring-shaped dysphotopsia.

Materials and Methods

Study population

This study was performed with approval from both the Institutional Review Board of Korea National Institute for Bioethics Policy and Korea University Ansan Hospital, Gyeonggi, Korea. All research and data collection adhered to the tenets of the Declaration of Helsinki and good clinical practices. The medical records of 15 consecutive myopic patients (29 eyes) who underwent hole ICL implantation at Joeeunnun Vision Clinic between January 2014 and July 2015 were retrospectively reviewed. Patients younger than 18 years, those who had previously undergone ocular surgery, those who had undergone additional corneal ablation surgeries to correct residual myopia or astigmatism and those who showed anterior segment abnormalities were excluded from the study (Lim et al. 2014).

Patient examination

All patients underwent comprehensive ophthalmic examination before surgery, including manifest and cycloplegic refraction, automated refraction and keratometry measured with an autorefractor/keratometer (ARK-700A; Nidek Co., Gamagori, Japan), uncorrected and best-corrected distance visual acuity, slit-lamp biomicroscopy, non-contact specular microscopy (SP-3000P; Topcon Corporation, Tokyo, Japan), corneal topography (Pentacam; Oculus Optikgeräte GmbH, Wetzlar, Germany and CT-1000; Shin-Nippon, Tokyo, Japan), analysis of pupil size under scotopic conditions (Colvard

pupillometer; Oasis Medical, Glendora, CA, USA), ultrasound pachymetry (Echoscan US-1800; Nidek Co.) and fundoscopic examination.

Implantable collamer lens power was calculated based on mean keratometry, central corneal thickness, horizontal white-to-white (WTW) distance, anterior chamber depth (ACD) and manifest refraction using the software provided by the manufacturer.

Patients were followed at 1 day, 2 weeks and 1, 2, 3 and 6 months after surgery. After that, follow-up appointments were made every 6–12 months. Patient perception of vision quality was evaluated using a questionnaire 1 month after surgery. Patients who experienced ring-shaped dysphotopsia were asked to evaluate whether and when ring-shaped dysphotopsia disappeared at each follow-up visit. Postoperative residual refractive error was measured at each follow-up visit.

Surgical technique

All hole ICL implantation procedures were performed by the same experienced surgeon (J.H.K.). After topical anaesthesia was achieved with proparacaine hydrochloride 0.5% (Alcaine; Alcon Laboratories Inc., Fort Worth, TX, USA), a 3.0-mm clear corneal incision was made on the steep axis,

and hydroxypropyl methylcellulose 2.0% (Eyefill® H.D., Croma-Pharma GmbH, Leobendorf, Austria) was injected into the anterior chamber. The hole ICL was implanted in the sulcus using a MicroSTAAR® injector (STAAR Surgical Co., Monrovia CA, USA). Approximately 0.3–0.6 ml of acetylcholine chloride (Miochol®-E, Bausch & Lomb, Rochester, NY,

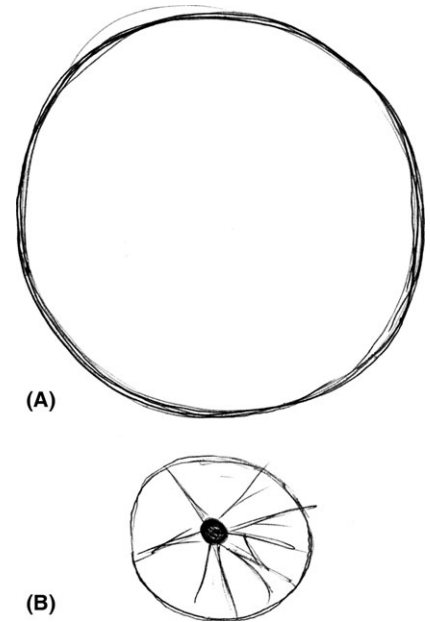


Fig. 1. Patient drawings representing (A) ring-shaped dysphotopsia; (B) glare.

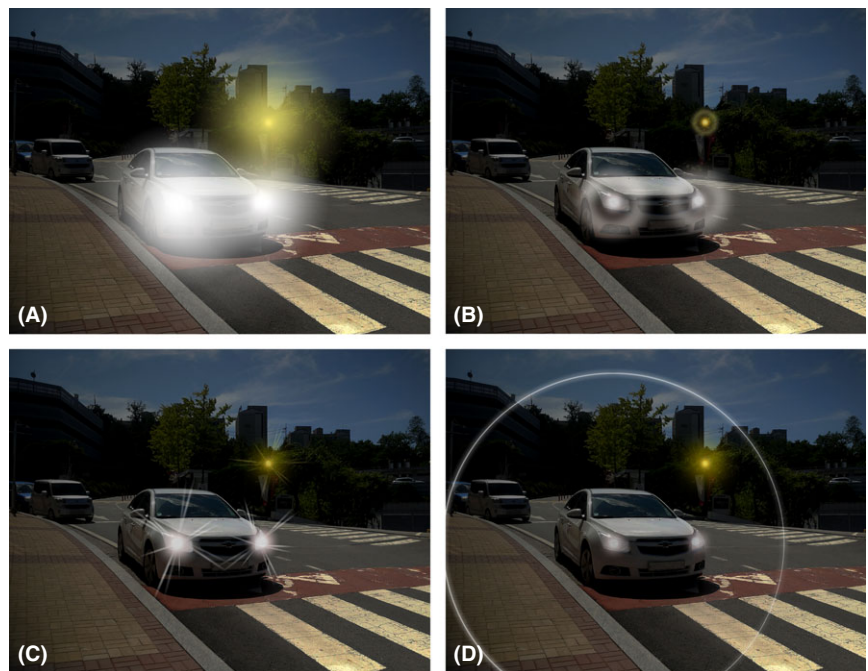


Fig. 2. Illustrations of glare, halos, starbursts and ring-shaped dysphotopsia used in the study questionnaire. (A) Glare; (B) Halos; (C) Starbursts; (D) Ring-shaped dysphotopsia.

USA) was injected into the anterior chamber. The anterior chamber was irrigated with a balanced salt solution to remove hydroxypropyl methylcellulose. The corneal incision was allowed to self-seal without any sutures.

Questionnaire

The incidence of glare, halos, starbursts and ring-shaped dysphotopsia was evaluated using a questionnaire with illustrations (McAlinden et al. 2010). An illustration for ring-shaped dysphotopsia was created in accordance with the statements of patients who previously experienced ring-shaped dysphotopsia to assist patients in distinguishing ring-shaped dysphotopsia from other visual disturbances (Fig. 2).

ICL-implanted eye modelling

A three-dimensional myopic human eye with a spectacle plane refraction of -10 dioptres at a vertex distance of 12 mm was modelled on the basis of the Arizona eye model (Greivenkamp et al. 1995; DeHoog & Doraiswamy 2014) using ZEMAX optical design software (Radiant Zemax, LLC, Redmond, WA, USA). A nominal ICL without a hole was located between the iris and the anterior crystalline lens surface. The entrance pupil diameter was set to 3.0 mm, and the ICL thickness was assumed to be 0.1 or 0.2 mm. The vault height was 0.4 mm for a 0.1-mm-thick ICL or 0.3 mm for a 0.2-mm-thick ICL. The shape of the ICL was optimized to correct myopic vision in the Zemax model.

The optimized ICL shape parameters were then used for non-sequential ray tracing for myopic human eyes with ICL in ASAP software. For the hole ICL case, a 0.36-mm-diameter central hole was generated. A rounded edge shape between the hole structure and the anterior and posterior ICL surfaces was applied with two different radius of curvature (ROC) values, 0.01 or 0.02 mm (Fig. 3). The ROC values of the hole edge were determined to resemble a pictorial cross section of the hole ICL in the brochure provided by the manufacturer (Medical International (medicalsintl.com). Ophthalmology: STAAR: Visian ICL with CentralFlow (V4C) Downloads. Available at: <http://www.medicalsintl.com/Content/uploads/Division/140617120248478~V4c%20Surgeon%20Brochure%20Final.pdf>. Accessed Aug 12, 2015.). The nominal human eye parameters used to model the ICL-implanted eye are presented in

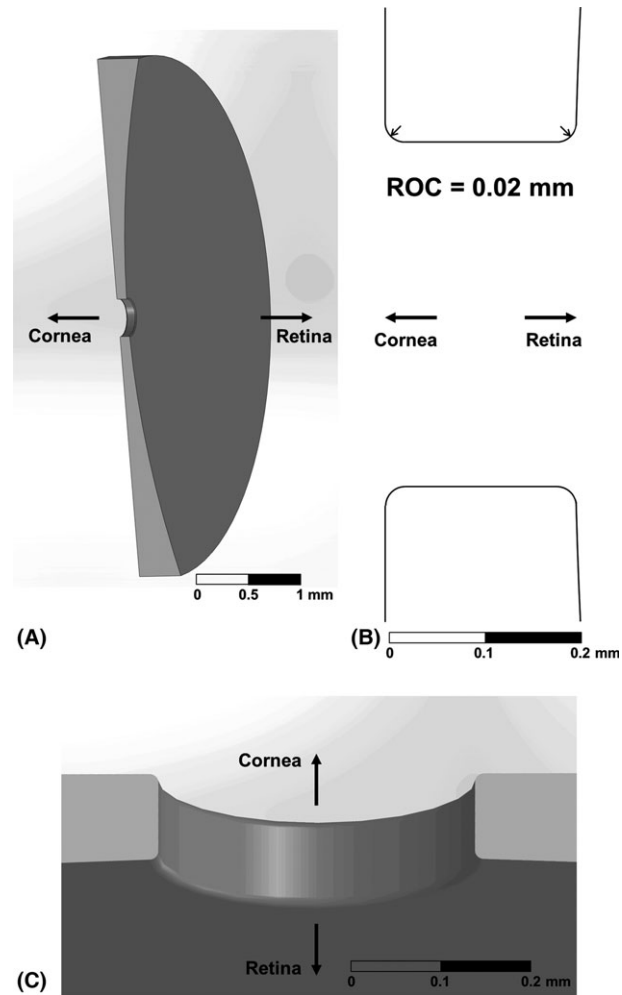


Fig. 3. A posterior chamber phakic implantable collamer lens (ICL) with a central hole (hole ICL), modelled in the Advanced Systems Analysis Program software. (A) Cross section of a hole ICL; (B) The radius of curvature (ROC) of the hole edge was 0.01 or 0.02 mm; (C) The rounded edge was applied at the interface between the central hole and the anterior and posterior ICL surfaces.

Table 1. The nominal values used in the study model of a posterior chamber phakic implantable collamer lens with or without a central hole.

Surface	Radius (mm)	Thickness (mm)	Conic	Refractive Index (at 546 nm wavelength)
Anterior cornea	7.800	0.550	-0.250	1.377
Posterior cornea	6.500	2.970	-0.250	1.337
Pupil	Infinity	0.000	0.000	1.337
Anterior ICL	Infinity	0.100 and 0.200	0.000	1.442
Posterior ICL	9.388 and 9.339	0.400 and 0.300	0.000	1.337
Anterior lens	12.000	3.767	-7.519	1.420
Posterior lens	-5.225	20.061	-1.354	1.336
Retina	-13.400	0.000	0.000	1.336

ICL = posterior chamber phakic implantable collamer lens.

Table 1. To identify only hole-induced dysphotopsia, an ideal conventional ICL was modelled in this study; the only difference between the conventional and hole ICLs was the physical hole itself.

Non-sequential ray tracing

Monochromatic analysis (light wavelength: 546 nm) was performed for all cases to prevent chromatic aberration-related effects, so that the simulation results only included stray light effects due to the central hole. The pupil irradiance was also fixed for all simulation cases. More than thirty million rays were traced for each case to produce statistically reliable results.

Every ray leaving the light-emitting object propagates independently until it interacts with any surface in the ICL-implanted eye. At the optical interface, the ray partially reflects and refracts based on the Fresnel equation until it meets another surface. This non-sequential ray tracing repeats until all the rays in the system reach their final surfaces. Once ray tracing is complete, information regarding ray spatial distribution on the retinal surface is obtained in terms of log-scale irradiance (normalized by the nominal peak value) and co-ordinate transformation is performed using MATLAB® (Matrix Laboratory, MathWorks, Inc., Natick, MA, USA) software in order for it to be displayed as retinal field angle. The retinal field angle was defined as 0° at the posterior pole and ±90° at the equatorial retina.

Stray light analysis

Imaging analysis

Ring-shaped dysphotopsia (simulation study 1): To compare vision quality between conventional and hole ICL-implanted eye models, an on-axis extended Lambertian light-emitting disc object 20 cm in diameter and 2 m from the corneal vertex was simulated. The on-axis extended Lambertian light source had a 2.9° half-cone angle and represented a typical lighting situation. The thickness of both ICLs used was 0.1 mm, and the ROC of the hole edge of the hole ICL was 0.01 mm. Two final retinal images were generated to compare the conventional and hole ICL cases. Detailed experimental simulation study parameters are summarized in Table 2.

Stray light pattern (simulation study 2): To investigate the fundamental mechanism of hole-induced ring-shaped dysphotopsia, a series of retinal images were simulated using point

Table 2. Experimental simulation study parameters used in the non-sequential ray-tracing analyses.

	Simulation 1	Simulation 2
Light source		
Wavelength (nm)	546	546
Type	Lambertian source	Collimated beam with 0, -1, -5, -10 and -20° field angle
Diameter (m)	0.2	Point
Distance (m)	2	Infinity
Numbers of rays*	30 000 000	90 000 000
Human eye		
Myopia (D)†	-10	-10
ICL		
Type	Conventional and hole ICLs	Hole ICL
Thickness (mm)	0.1	0.1 and 0.2
ROC of the hole edge (mm)	0.01	0.01 and 0.02

D = dioptres; ICL = posterior chamber phakic implantable collamer lens; Conventional ICL = ICL without a central hole; Hole ICL = ICL with a 0.36 mm central hole; ROC = radius of curvature.

* Numbers of rays traced for each simulation.

† Spectacle plane refraction at a vertex distance of 12 mm.

sources at infinity with well-defined field angles (0, -1, -5, -10 and -20°). Each field angle case produced a corresponding retinal image pattern representing the stray light pattern caused by the inner wall of the central hole. In other words, the ring-shaped dysphotopsia in simulation study 1 was a superposition of these corresponding retinal image patterns. Various ICL configurations (ICL thickness: 0.1 and 0.2 mm; ROC of the hole edge: 0.01 and 0.02 mm) were analysed to draw more generic conclusions (Table 2).

Radiometric analysis

To verify the non-sequential ray tracing used in this study, the ratio of radiant power of stray light to total light in the hole ICL-implanted eye (ICL thickness: 0.1 mm; ROC of the hole edge: 0.01 mm) was calculated according to the angle of incidence of the light rays from 0 to 50° at 5° intervals. Ten thousand rays were traced for each angle of incidence, and ray tracing was repeated 1000 times under the same conditions to calculate standard deviation (SD).

Statistical analysis

We used SPSS version 12.0 (SPSS, Inc., Chicago, IL, USA) for all descriptive statistics of patient data. Mann-Whitney *U*-tests were performed for the statistical comparison of preoperative and postoperative variables and ICL parameters between eyes with and

without ring-shaped dysphotopsia. Pearson χ^2 tests were performed to compare the incidence of glare, halos and starbursts between eyes with and without ring-shaped dysphotopsia. *p* values <0.05 were considered statistically significant.

Results

Clinical study

The mean patient age was 24.3 ± 4.1 years (range, 19 to 33 years). Of 15 patients, six were men. The mean implanted ICL power was -10.2 ± 2.8 D (range, -16.5 to -4.0 D). Table 3 presents other parameters, including laterality, preoperative refractive errors, ICL size and follow-up period.

Of 29 total eyes, 18 (62.1%) experienced glare with the mean duration of 3.0 ± 3.4 months (range, 1–12 months), 16 (55.2%) experienced halos with the mean duration of 3.1 ± 3.6 months (range, 1–12 months), 10 (34.5%) experienced starbursts with the mean duration of 1.8 ± 0.8 months (range, 1–3 months) and 15 (51.7%) experienced ring-shaped dysphotopsia with the mean duration of 2.9 ± 3.8 months (range, 1–12 months) after hole ICL implantation. There were no significant differences in age, preoperative and postoperative variables, ICL parameters, the incidence of halos and starbursts, or the duration of glare, halos and starbursts between eyes with and without ring-shaped dysphotopsia. However, the incidence of glare

was significantly higher in eyes with ring-shaped dysphotopsia than in eyes without ring-shaped dysphotopsia (Table 4).

Imaging analysis

Ring-shaped dysphotopsia (simulation study 1)

The conventional ICL showed a well-demarcated, round image at the foveal centre (Fig. 4A). On the other hand, the hole ICL-evoked glare and ring-shaped dysphotopsia located near the $\pm 40^\circ$ retinal field angle. The relative normalized irradiance of the ring-shaped dysphotopsia ($10^{-3.9}$) was approximately 8000-fold less than the peak irradiance at the nominal focus location (10^0) in the hole ICL (Fig. 4B).

Stray light pattern (simulation study 2)

The source of the ring-shaped stray light pattern was depicted in the two non-sequential ray-tracing plots (using collimated input rays with a -10° angle of incidence of the light ray) comparing the conventional ICL with the hole ICL case. While the conventional ICL focused all of the rays on a single point, the hole ICL produced arc patterns on the retina (Fig. 5A). Stray light (the red rays in Fig. 5B) was created by light refraction from the inner wall of the hole and the anterior and posterior ICL surfaces.

Figure 6 presents the final retinal images measured in log-scale irradiance for multiple field angles ($0, -1, -5, -10$ and -20°) through hole ICL-implanted eyes. For all of the field angles, the stray light pattern was clearly observed within a typical human eye dynamic range (irradiance difference range from 10^0 to 10^{-9}). There were two main patterns: glare and arc images. For the 0.1-mm-thick hole ICL case with a 0.01-mm ROC of the hole edge, the relative normalized irradiance of the glare and arc pattern (10^{-5}) was approximately 100 000-fold less than that at the nominal focus location (10^0). The size of the pattern generally increased as the field angle increased.

The location of the ring-shaped dysphotopsia associated with hole ICL (Fig. 4B) mainly corresponded to the arc pattern (for the 0.1-mm-thick hole ICL with a 0.01-mm ROC of the hole edge) for the -5° field angle case (Fig. 6). These results demonstrated

Table 3. Clinical characteristics of patients and study eyes who underwent ICL with a central hole (29 eyes of 15 patients).

Parameter	Mean \pm SD	Range
Age, years	24.3 \pm 4.1	19, 33
Sex, <i>n</i>		
Male (%)	6 (40.0)	–
Female (%)	9 (60.0)	–
Laterality, <i>n</i>		
Right eye (%)	15 (51.7)	–
Left eye (%)	14 (48.3)	–
Preoperative refractive errors, D	-9.30 ± 2.66	$-15.50, -3.00$
ICL power, D	-10.2 ± 2.8	$-16.5, -4.0$
ICL size, mm	12.4 ± 0.3	12.1, 13.2
Follow-up period, months	4.5 ± 4.1	1, 12

SD = standard deviation; D = dioptres; ICL = implantable collamer lens.

Table 4. Comparison of preoperative and postoperative variables; implantable collamer lens parameters; and the incidence of other visual disturbances.

	Eyes with ring-shaped dysphotopsia (<i>n</i> = 15) (Mean \pm SD)	Eyes without ring-shaped dysphotopsia (<i>n</i> = 14) (Mean \pm SD)	p value*
Age, years	25.2 \pm 4.1	23.3 \pm 4.0	0.217
Preoperative data			
Corneal power, D	43.69 \pm 1.24	43.39 \pm 1.23	0.425
Corneal cylinder power, CD	1.65 \pm 0.68	2.02 \pm 0.58	0.134
White-to-white diameter, mm	11.3 \pm 0.3	11.2 \pm 0.3	0.621
Central corneal thickness, mm	520.2 \pm 36.9	528.4 \pm 28.2	0.533
Anterior chamber depth, mm	3.20 \pm 0.16	3.21 \pm 0.12	0.780
Pupil size, mm	7.0 \pm 0.7	7.0 \pm 0.9	0.880
Postoperative data			
Residual refractive errors, D			
Spherical	0.38 \pm 0.35	0.61 \pm 0.23	0.077
Cylindrical	-1.22 ± 0.31	-1.30 ± 0.57	0.715
Spherical equivalent	-0.23 ± 0.37	-0.05 ± 0.32	0.217
UDVA, logMAR	0.00 \pm 0.00	0.04 \pm 0.05	0.051
ICL power, D	-9.7 ± 3.5	-10.8 ± 1.6	0.310
ICL size, mm	12.4 \pm 0.4	12.4 \pm 0.3	0.880
Visual disturbances			
Glare, <i>n</i>			
Yes (%)	12 (80.0)	6 (42.9)	0.039 [†]
No (%)	3 (20.0)	8 (57.1)	
Halos, <i>n</i>			
Yes (%)	10 (66.7)	6 (42.9)	0.198 [†]
No (%)	5 (33.3)	8 (57.1)	
Starbursts, <i>n</i>			
Yes (%)	6 (40.0)	4 (28.6)	0.518 [†]
No (%)	9 (60.0)	10 (71.4)	
Duration of visual disturbances			
Glare, months	3.5 \pm 4.0	2.0 \pm 0.9	0.892
Halos, months	3.6 \pm 4.5	2.3 \pm 1.0	0.562
Starbursts, months	2.0 \pm 0.9	1.5 \pm 0.6	0.476

D = dioptres; CD = cylinder dioptres; UDVA = uncorrected distance visual acuity; ICL = implantable collamer lens.

* Calculated with Mann–Whitney *U*-test.

[†] Calculated with Pearson χ^2 test.

that the convolution of stray light patterns created by the rays leaving the extended Lambertian source within 0 to $\pm 2.9^\circ$ ray angles with respect to the optical axis contributed to the ring-shaped dysphotopsia pattern on the retina.

A zoomed-in, stray light ray path showed that the arc patterns that form ring-shaped dysphotopsia on the retina were created by rays meeting the inner wall of the hole structure and the posterior ICL surface (Fig. 7).

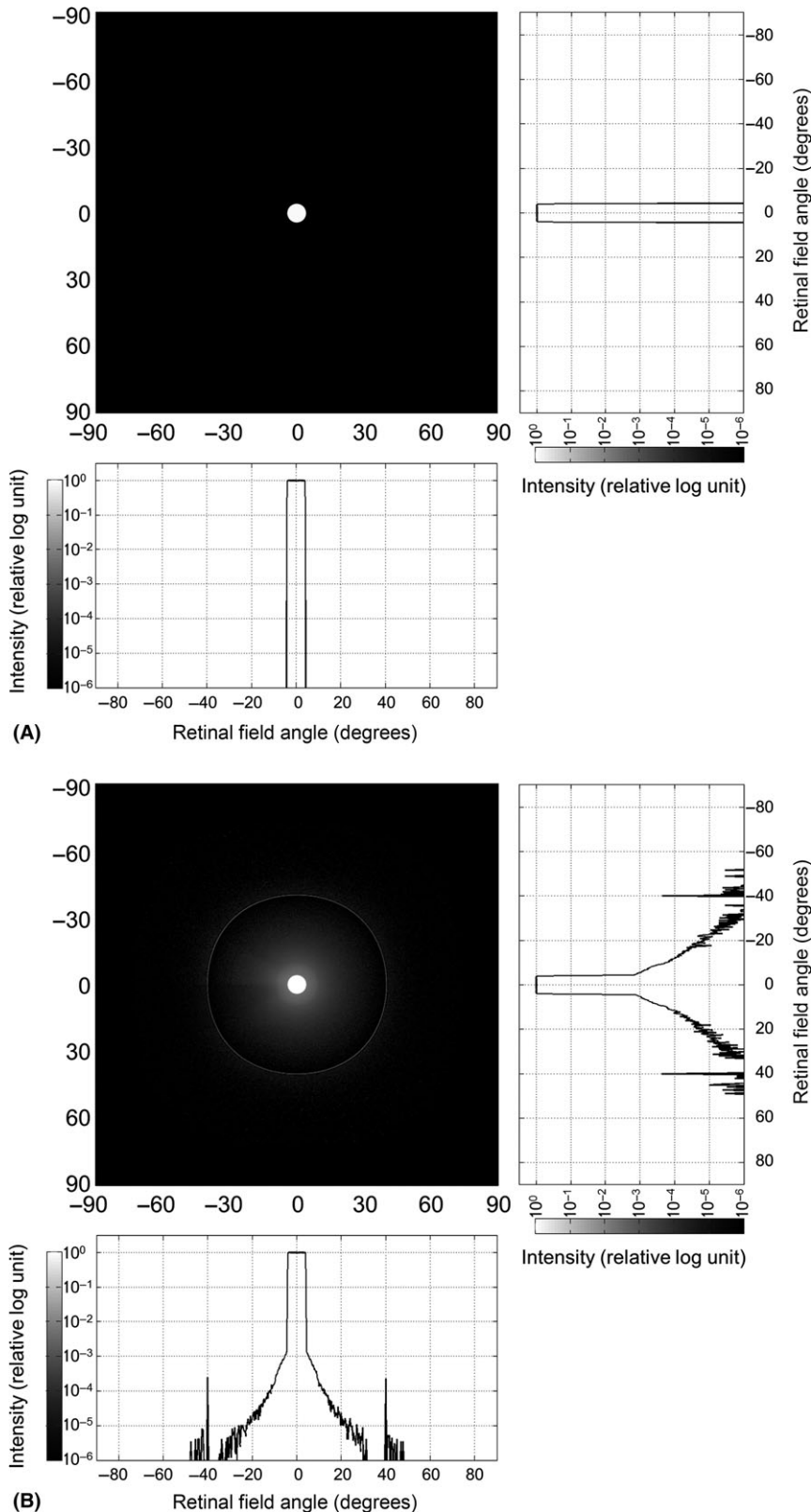


Fig. 4. Retinal images measured as normalized log-scale irradiances of the myopic human eye model (spectacle plane refraction of -10 dioptres at a vertex distance of 12 mm) corrected with a conventional posterior chamber phakic implantable collamer lens (ICL) and a hole ICL on non-sequential ray tracing using an extended Lambertian light-emitting disc object 20 cm in diameter and 2 m from the corneal vertex. A nominal value for ICL thickness of 0.1 mm was used for both conventional and hole ICLs, and the radius of curvature of the hole edge was 0.01 mm for the hole ICL. (A) The conventional ICL showed a well-demarcated round image at the foveal centre; (B) The hole ICL produced glare and ring-shaped dysphotopsia at a retinal field angle of $\pm 40^\circ$.

Radiometric analysis

The ratio of radiant power of stray light to total light rays increased as the angle of incidence of the light rays increased. The calculated SDs were in the range of 0.004 – 0.071% (Fig. 8).

Discussion

In this study, 51.7% of the examined eyes experienced ring-shaped dysphotopsia after hole ICL implantation. Previous studies that compared optical quality between conventional and hole ICLs did not document ring-shaped dysphotopsia (Shimizu et al. 2012; Alfonso et al. 2013; Ferrer-Blasco et al. 2013; Kamiya et al. 2013). Upon hearing about ring-shaped dysphotopsia for the first time from patients who underwent hole ICL surgery, we assumed that the ring-shaped dysphotopsia mentioned was small in size and similar to halos seen in other conditions. However, when patients described the disturbance in detail and illustrated their symptoms in drawings, it became clear that ring-shaped dysphotopsia was a distinct symptom. Previous studies might have failed to note ring-shaped dysphotopsia after hole ICL surgery because it was unexpected (Shimizu et al. 2012; Alfonso et al. 2013; Ferrer-Blasco et al. 2013; Kamiya et al. 2013). We designed images to help patients distinguish ring-shaped dysphotopsia from other visual disturbances and showed that hole ICL could evoke ring-shaped dysphotopsia. To the best of our knowledge, this is the first clinical report describing ring-shaped dysphotopsia after hole ICL implantation.

To investigate central hole-induced dysphotopsia, this study compared simulated retinal images between conventional and hole ICLs using a non-sequential ray-tracing method. Non-sequential ray tracing was successfully used to estimate the cause of hole-induced ring-shaped dysphotopsia. It is important to note that the described hole-induced stray light was mainly produced by refraction from the hole structure. In particular, this occurs more evidently in situations where light rays pass obliquely through the central hole. Eppig et al. (2015) showed that the central hole of hole ICL may be a source of positive dysphotopsia using a non-sequential ray-tracing method. In

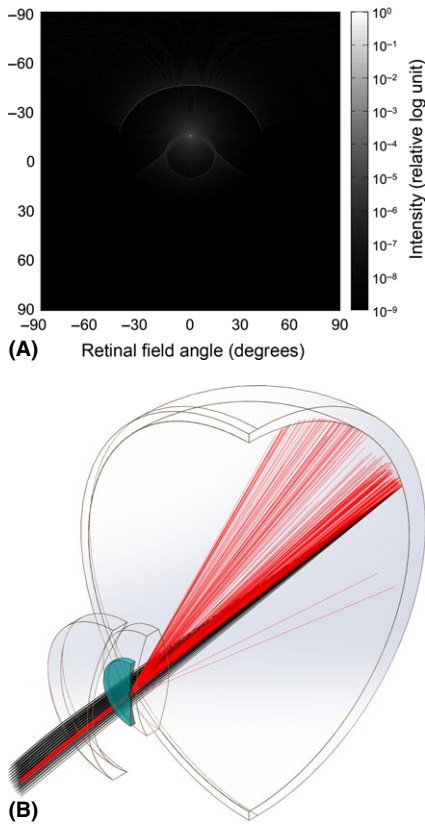


Fig. 5. Non-sequential ray tracing using parallel light rays in a myopic human eye model (spectacle plane refraction of -10 dioptres at a vertex distance of 12 mm) with a posterior chamber phakic implantable collamer lens (ICL) with a central hole (hole ICL). The nominal value for ICL thickness was 0.1 mm, and the radius of curvature of the hole edge was 0.01 mm. (A and B) The hole ICL produces an arc and ring images caused by light refraction from the inner wall of the central hole and the posterior ICL surface.

that study, positive dysphotopsia mainly originated from light reflection from the inner wall of the central hole. For some specific lighting situations, the light entering the central hole may be prone to high reflection, such as total internal reflection, which depends on polarization status and incident angle.

In contrast to the results of this study, previous studies comparing modulation transfer function (MTF), wavefront aberration, point spread function (PSF) or the objective scatter index between conventional and hole ICLs did not show meaningful differences in these factors and could not predict ring-shaped dysphotopsia. Modulation transfer function (MTF) is one of the most commonly used methods for evaluating optical system performance such as the preclinical evaluation of new

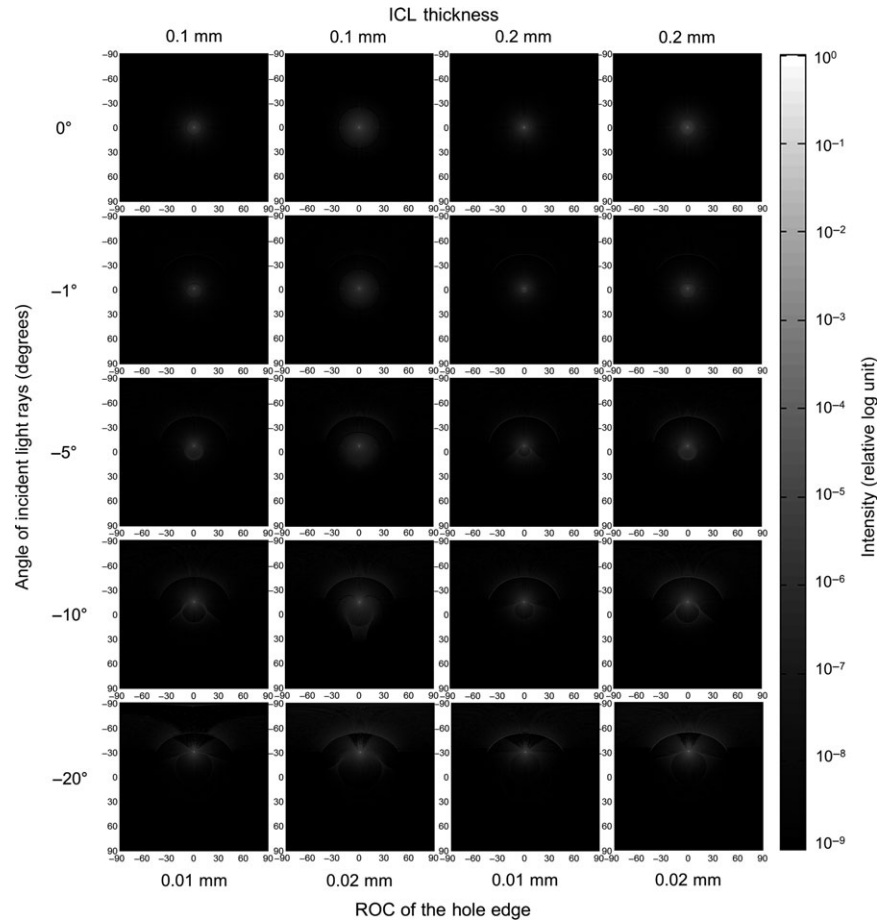


Fig. 6. Retinal images measured as normalized log-scale irradiances of the myopic human eye model (spectacle plane refraction of -10 dioptres at a vertex distance of 12 mm) with a posterior chamber phakic implantable collamer lens (ICL) with a central hole on non-sequential ray tracing using collimated rays according to the angle of incident light rays (0 , -1 , -5 , -10 and -20°) at an ICL thickness of 0.1 or 0.2 mm and a 0.01 - or 0.02 -mm radius of curvature (ROC) of the hole edge.

intraocular lenses and design changes (Lang et al. 1993). However, in previous study, there were no differences in MTF between conventional and hole ICLs, or the MTF differences were small enough to be clinically negligible (Shiratani et al. 2008; Uozato et al. 2011). In addition, Perez-Vives et al. (2013) also showed that hole ICL has comparable optical quality in terms of both wavefront aberration and PSF with respect to conventional ICLs. Several previous studies that compared objective scatter indices reported no meaningful differences between conventional and hole ICLs (Kamiya et al. 2013; Huseynova et al. 2014). These previous studies on image quality in hole ICLs failed to predict central hole related any dysphotopsia, as they mostly measured on-axis quality without any glare or off-axis lighting. In addition, it seems that these analyses (MTF, wavefront aberration, PSF and objective scatter index) are not

appropriate methods for investigating central hole-induced dysphotopsia in hole ICL-implanted eyes.

The results of this study successfully demonstrated that hole ICL evoked glares and ring-shaped dysphotopsias under experimental conditions using the extended Lambertian source, which is a good simplified approximation of light sources in daily life. Component-level analysis was used to investigate individual stray light patterns of hole ICLs for a collimated input beam with various field angles. The clinically reported (Fig. 1) or simulated (Fig. 4B) ring-shaped dysphotopsia is the convolution of each individual stray light pattern with the light source's spatial and angular distribution. As shown in Fig. 6, the stray light pattern is a complex function of the light source and ICL configuration and requires case-by-case simulation. However, the convolution of stray light

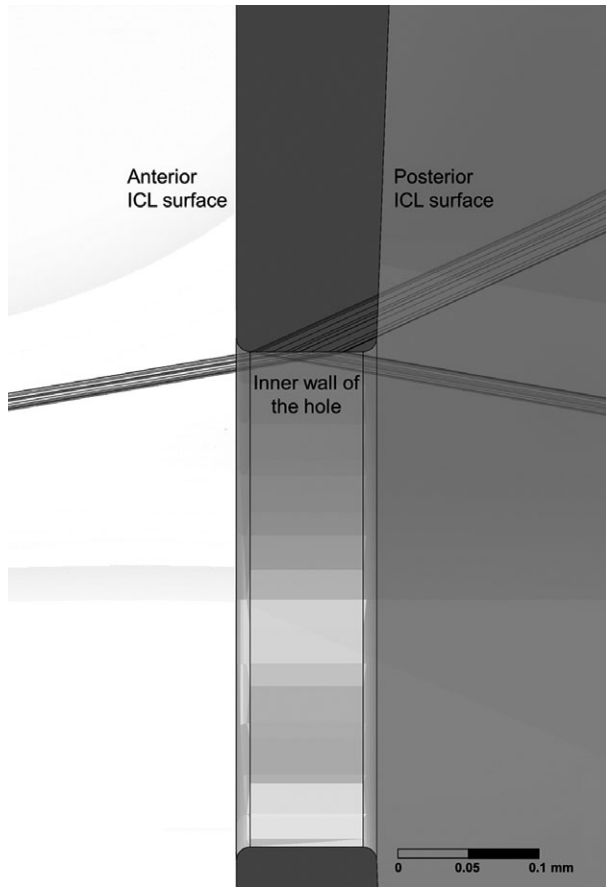


Fig. 7. A zoomed-in stray light ray path showing that arc patterns that form the entire ring-shaped dysphotopsia pattern on the retina are created by rays meeting the inner wall of the hole structure of a posterior chamber phakic implantable collamer lens (ICL).

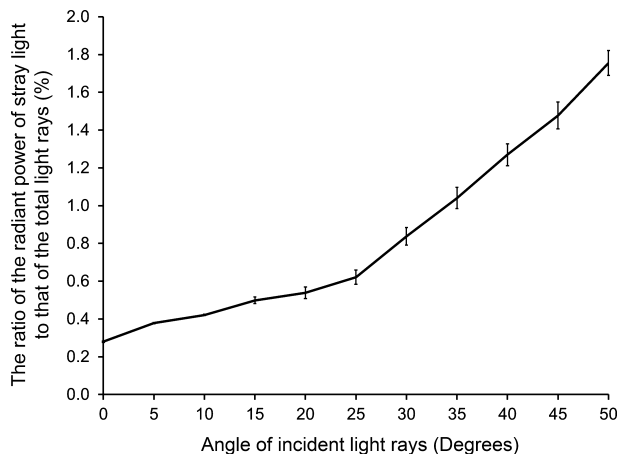


Fig. 8. The ratio of radiant power of stray light to total light rays in the myopic human eye model (spectacle plane refraction of -10 dioptres at a vertex distance of 12 mm) with a posterior chamber phakic implantable collamer lens (ICL) with a central hole (ICL thickness: 0.1 mm; radius of curvature of the hole edge: 0.01 mm) on non-sequential ray tracing using collimated rays according to an angle of incidence from 0 to 50° at 5° intervals.

patterns generally forms characteristic ring-like shapes. This provides an adequate explanation for general observations regarding the patients reported in this study.

When selecting an ICL, it is necessary to consider various aspects of the two available types. In the case of hole ICL, surgeons should inform patients about the possibility of experiencing

ring-shaped dysphotopsia. However, hole ICL has the possible advantages of improved aqueous humour circulation (Fujisawa et al. 2007), reduced cataract formation (Shiratani et al. 2008) and decreased need for preoperative laser peripheral iridotomy, although long-term studies on these advantages are not yet available. In addition, a previous study demonstrated that a central hole diameter of 0.36 mm is close to the ideal hole size in hole ICL from the standpoint of the fluid dynamics of the aqueous humour (Kawamorita et al. 2016). Thus, despite central hole-induced dysphotopsia, when considering all of the advantages and disadvantages for a given patient's situation, hole ICL might remain an attractive solution over conventional ICL.

There are some limitations to this study. First, a refractive index of 1.442 was assumed for the ICLs. The hydrophilic Collamer[®] (STAAR Surgical Co.) lens material has a high water content layer on the surface, and its actual refractive index varies as a function of location in the lens. This assumption affects the amount of Fresnel reflection from the interface, which might affect the amplitude of the retinal image irradiance. However, it does not affect the ring-shaped irradiance pattern, which was the main focus of this stray light analysis. Second, the rounded edge design of the central hole might be slightly different from that of the hole ICL. Because stray light is related to the entire hole structure rather than just the rounded edge, the effects of edge redesign would be negligible.

In conclusion, the central hole of hole ICL can be a source of glare and ring-shaped dysphotopsia. Ring-shaped dysphotopsia is caused by the merging of arc images caused by obliquely incident light. In daily life, a person is often exposed to oblique lighting conditions, and, even in the case of on-axis light sources placed in the direction of the visual axis, most lights are oblique rays. Surgeons should advise patients considering hole ICL implantation of the possibility of central hole-induced ring-shaped dysphotopsia.

References

Alfonso JF, Baamonde B, Fernandez-Vega L, Fernandes P, González-Méijome JM &

- Montés-Micó R (2011): Posterior chamber collagen copolymer phakic intraocular lenses to correct myopia: five-year follow-up. *J Cataract Refract Surg* **37**: 873–880.
- Alfonso JF, Lisa C, Fernandez-Vega Cueto L, Belda-Salmerón L, Madrid-Costa D & Montés-Micó R (2013): Clinical outcomes after implantation of a posterior chamber collagen copolymer phakic intraocular lens with a central hole for myopic correction. *J Cataract Refract Surg* **39**: 915–921.
- DeHoog E & Doraiswamy A (2014): Evaluation of the impact of light scatter from glisterings in pseudophakic eyes. *J Cataract Refract Surg* **40**: 95–103.
- Donnelly W 3rd (2008): The Advanced Human Eye Model (AHM): a personal binocular eye modeling system inclusive of refraction, diffraction, and scatter. *J Refract Surg* **24**: 976–983.
- Eppig T, Spira C, Tsintarakis T, El-Husseiny M, Cayless A, Müller M, Seitz B & Langenbucher A (2015): Ghost-image analysis in phakic intraocular lenses with central hole as a potential cause of dysphotopsia. *J Cataract Refract Surg* **41**: 2552–2559.
- Ferrer-Blasco T, Garcia-Lazaro S, Belda-Salmeron L, Albarrán-Diego C & Montés-Micó R (2013): Intra-eye visual function comparison with and without a central hole contact lens-based system: potential applications to ICL design. *J Refract Surg* **29**: 702–707.
- Fujisawa K, Shimizu K, Uga S, Suzuki M, Nagano K, Murakami Y & Goseki H (2007): Changes in the crystalline lens resulting from insertion of a phakic IOL (ICL) into the porcine eye. *Graefes Arch Clin Exp Ophthalmol* **245**: 114–122.
- Gonvers M, Bornet C & Othenin-Girard P (2003): Implantable contact lens for moderate to high myopia: relationship of vaulting to cataract formation. *J Cataract Refract Surg* **29**: 918–924.
- Greivenkamp JE, Schwiegerling J, Miller JM & Mellinger MD (1995): Visual acuity modeling using optical raytracing of schematic eyes. *Am J Ophthalmol* **120**: 227–240.
- Huseynova T, Ozaki S, Ishizuka T, Mita M & Tomita M (2014): Comparative study of 2 types of implantable collamer lenses, 1 with and 1 without a central artificial hole. *Am J Ophthalmol* **157**: 1136–1143.
- Kamiya K, Shimizu K, Saito A, Igarashi A & Kobashi H (2013): Comparison of optical quality and intraocular scattering after posterior chamber phakic intraocular lens with and without a central hole (Hole ICL and Conventional ICL) implantation using the double-pass instrument. *PLoS ONE* **8**: e66846.
- Kawamorita T, Shimizu K & Shoji N (2016): Effect of hole size on fluid dynamics of a posterior-chamber phakic intraocular lens with a central perforation by using computational fluid dynamics. *Graefes Arch Clin Exp Ophthalmol* **254**: 739–744.
- Lang AJ, Lakshminarayanan V & Portney V (1993): Phenomenological model for interpreting the clinical significance of the in vitro optical transfer function. *J Opt Soc Am A* **10**: 1600–1610.
- Lim DH, Lyu IJ, Choi SH, Chung ES & Chung TY (2014): Risk factors associated with night vision disturbances after phakic intraocular lens implantation. *Am J Ophthalmol* **157**: 135–141 e131.
- McAlinden C, Pesudovs K & Moore JE (2010): The development of an instrument to measure quality of vision: the Quality of Vision (QoV) questionnaire. *Invest Ophthalmol Vis Sci* **51**: 5537–5545.
- Medical International (medicalsintl.com). Ophthalmology: STAAR: Visian ICL with CentralFlow (V4C) Downloads. Available at: <http://www.medicalsintl.com/Content/uploads/Division/140617120248478-V4c%20Surgeon%20Brochure%20Final.pdf>. Accessed Aug 12, 2015.
- Perez-Vives C, Ferrer-Blasco T, Madrid-Costa D, Garcia-Lázaro S & Montés-Micó R (2013): Optical quality comparison of conventional and hole-visian implantable collamer lens at different degrees of decentration. *Am J Ophthalmol* **156**: 69–76 e61.
- Sanders DR, Vukich JA, Doney K, Gaston M & Implantable Contact Lens in Treatment of Myopia Study Group (2003): US food and drug administration clinical trial of the implantable contact lens for moderate to high myopia. *Ophthalmology* **110**: 255–266.
- Shimizu K, Kamiya K, Igarashi A & Shiratani T (2012): Intraindividual comparison of visual performance after posterior chamber phakic intraocular lens with and without a central hole implantation for moderate to high myopia. *Am J Ophthalmol* **154**: 486–494 e481.
- Shiratani T, Shimizu K, Fujisawa K, Uga S, Nagano K & Murakami Y (2008): Crystalline lens changes in porcine eyes with implanted phakic IOL (ICL) with a central hole. *Graefes Arch Clin Exp Ophthalmol* **246**: 719–728.
- Uozato H, Shimizu K, Kawamorita T & Ohmoto F (2011): Modulation transfer function of intraocular collamer lens with a central artificial hole. *Graefes Arch Clin Exp Ophthalmol* **249**: 1081–1085.

Received on February 3rd, 2016.
Accepted on July 25th, 2016.

Correspondence:

Hyo Myung Kim, MD, PhD
Department of Ophthalmology
Anam Hospital, Korea University College of Medicine
126-1, Anam-dong 5-ga, Seongbuk-gu
Seoul 136-705
South Korea
Tel: +82 2 920 5776
Fax: +82 2 924 6820
Email: hyomkim@kumc.or.kr

Publication of this article was supported in part by the SRC Program (2010-0027910) of the Center for Galaxy Evolution Research (CGER), by the Korea Astronomy and Space Science Institute under the R&D program (Project No. 2014-9-710-03) supervised by the Ministry of Science, ICT and Future Planning, South Korea, and by the Busan Sungmo Eye Hospital Sodam scholarship committee. The authors would like to acknowledge the support of the Breault Research Organization through user licences for the Advanced System Analysis Program (ASAP™) for ray-tracing computation. The authors would also like to thank web designer Ye Jin Jang for the illustrations used in the study questionnaire.

This work was presented in part at the annual meeting of the Korean Society of Cataract and Refractive Surgery (KSCRS), Seoul, South Korea, July 13, 2014; the 112th Meeting of the Korean Ophthalmological Society, Gyeonggi-do, South Korea, October 31–November 2, 2014; the Asia-Association for Research in Vision and Ophthalmology (ARVO), Yokohama, Japan, February 16–19, 2015; and at XXXIII congress of the European Society of Cataract & Refractive Surgeons (ESCRS), Barcelona, Spain, September 5–9, 2015.